



Published in final edited form as:

*J Neurol Transl Neurosci*. 2014 ; 2(1): .

## Deletion of Virus-specific T-cells Enhances Remyelination in a Model of Multiple Sclerosis

Aleksandar Denic<sup>1</sup>, Bharath Wootla<sup>1</sup>, Laurie Zoecklein<sup>1</sup>, and Moses Rodriguez<sup>1,2,\*</sup>

<sup>1</sup>Department of Neurology, Mayo Clinic, Rochester, MN 55905

<sup>2</sup>Department of Immunology, Mayo Clinic, Rochester, MN 55905

### Abstract

We used transgenic expression of capsid antigens to Theiler's murine encephalomyelitis virus (TMEV) to study how the immune response to VP1 and VP2 influences spinal cord demyelination, remyelination and axonal loss during the acute and chronic phases of infection. Expression from birth of capsid antigen under the ubiquitin promoter resulted in tolerance to the antigen and absence of an immune response to the respective capsid antigen following virus infection. The transgenic mice were crossed to B10.Q mice normally susceptible to demyelination but which, when compared to FVB mice of the same H2<sup>d</sup> haplotype, show poor remyelination. The major finding in this study was that VP1<sup>+</sup> and VP2<sup>+</sup> animals featured more remyelination at all three chronic time points (90, 180 and 270 dpi) than transgene-negative controls. Interestingly, at 270 dpi, remyelination in VP1<sup>+</sup> mice tended to be higher and more complete than that in VP2<sup>+</sup> mice. Compared with transgene-negative controls, VP1<sup>+</sup> and VP2<sup>+</sup> animals showed similar demyelination in but less only late in the disease (270 dpi). The number of mid-thoracic axons at the last time point correlated with the levels of remyelination. The increase in number of axons in VP1<sup>+</sup> mice with remyelination was driven by counts in medium- and large-caliber axons. This study supports the hypothesis that expression of viral capsid proteins as self and subsequent genetic deletion of capsid-specific T cells influences the extent of spinal cord remyelination following Theiler's virus-induced demyelination. We propose that VP1<sup>-</sup> and, to a lesser extent, VP2-specific CD8<sup>+</sup> T cells limit and/or prevent the naturally occurring process of remyelination. This finding may have relevance to human multiple sclerosis, as targeted removal of CD8<sup>+</sup> T cells specific for a yet-to-be-discovered causative peptide may enhance remyelination and prevent axonal loss in patients.

### Keywords

VP1; VP2; TMEV; Remyelination; Axons; Multiple Sclerosis

### Introduction

Multiple sclerosis (MS) is a disease of the central nervous system (CNS) with varied clinical presentations and heterogeneous histopathological features. Inflammatory demyelination is a

\*Corresponding author: Moses Rodriguez, MD, Department of Neurology, Mayo Clinic, 200 First St. SW, Rochester, MN, 55905, Phone: (507) 284-4663, Fax: (507) 284-1086, rodriguez.moses@mayo.edu.

prominent feature of MS. Demyelination is the pathological process wherein axons lose their protective myelin sheaths. Lipid-rich myelin sheaths surround axons and aid in efficient saltatory propagation of action potentials. CNS tissue can repair itself after injury either through a scar formation or regeneration. Scar formation by astrocytes usually predominates; however, occasional remyelination in MS offers a striking example of robust CNS regeneration [1]. Remyelination involves reinvesting demyelinated axons with new myelin sheaths. This has been described in MS as well as in a number of experimental disease models [2, 3]. MS represents one of the most common causes of neurological disability in young adults in the Western world, and to date, there is neither a definitive cause nor an effective cure.

Different animal models of MS were developed in order to understand the disease process. Lysolecithin- and cuprizone-induced demyelination models were designed to study processes of focal remyelination [4]. Lysolecithin is an activator of phospholipase A2, and cuprizone is a copper chelator. The most widely used animal model in MS research is the experimental autoimmune encephalomyelitis (EAE). The immune system is considered a major culprit in MS pathogenesis, and the EAE model provides means to study the role of the immune system in disease progression. However, EAE is driven by Th-1 CD4<sup>+</sup> T cells and IL-17 and thus, for several decades, MS research has focused on this subset of T cells. Numerous ineffective or, in some cases, even harmful novel therapeutic trials based on results from EAE studies [5, 6] led researchers to investigate alternative mechanisms for MS pathogenesis. In addition, recent landmark studies in MS lesion samples highlighted CD8<sup>+</sup> T cells as major players in human MS [7, 8].

Our laboratory uses the Theiler's murine encephalomyelitis virus (TMEV)-induced demyelinating disease [9]. TMEV is a positive-stranded RNA virus belonging to the family *Picornaviridae*. Intracranial infection with TMEV leads to an encephalitis that is resolved in most strains of mice; however, certain strains develop chronic infection and demyelination in the spinal cord white matter. TMEV-induced demyelinating disease emphasizes a role of primarily CD8<sup>+</sup> T cells [10–12]. We showed previously that the immune system is important in protecting mice from virus-induced demyelination. We generated lines of transgenic B10 mice (on resistant H-2<sup>b</sup> background) expressing three independent contiguous coding regions of TMEV under the control of a class I MHC promoter. Normally, TMEV infection of resistant B10 mice results in acute encephalitis, but the virus is cleared within 3 weeks without chronic demyelination or persistent neurological deficits. However, when viral capsid genes were transgenically expressed, it resulted in deletion of only virus-specific CD8<sup>+</sup> T cells directed against the relevant peptides but did not alter production of virus-specific antibodies or CD4<sup>+</sup> T-cells [13]. Following intracerebral infection with TMEV, we found that VP1-positive (VP1+) transgenic mice developed virus persistence and subsequent demyelination in spinal cord white matter [13]. Interestingly, transgenic mice expressing non-capsid proteins cleared the virus and did not develop demyelination. This study suggested that deletion of specific CD8<sup>+</sup> T cells by ubiquitous expression of relevant virus capsid peptides inhibited resistance to virus-induced demyelination. Taken together, this data support the hypothesis that the immune responses to TMEV capsid proteins contribute

to the pathogenesis of TMEV infection and are critical in determining resistance vs. susceptibility to immune-mediated demyelination.

There is also evidence for the contribution of CD8<sup>+</sup> T cell-mediated immune response that leads to demyelination and neurologic deficits in susceptible strains of mice. When susceptible mice were pre-immunized with VP1 or VP2 proteins, demyelination was absent; however, immunization with VP3 caused demyelination, suggesting that an immune response to VP1 and VP2 proteins was beneficial [14]. More recently, using the transgenic approach, we demonstrated that compared to wild type FVB mice, transgenic expression of TMEV capsid proteins VP1, VP2 and epitope VP2<sub>121-130</sub> worsened spinal cord pathology and caused more axonal loss [15]. The effect was more pronounced in VP2 and VP2<sub>121-130</sub> transgenic animals. Interestingly, the viral load was similar in wild type and all three transgenic strains. The study focused on the role of various capsid-specific CD8<sup>+</sup> T cells and their contribution to demyelination and axonal loss. During the chronic phase of TMEV-induced demyelinating disease, FVB mice exhibit remarkable remyelination and axonal preservation [16]. Indeed, we observed similar levels of remyelination in FVB wild type and all TMEV transgenic strains (unpublished data).

Multiple studies suggest that CD8<sup>+</sup> T-cells represent a factor that restricts remyelination. A major obstacle to remyelination research in human MS is the inability to identify the target antigen(s) that cause MS. Such knowledge would aid in designing a therapy that would specifically delete an antigen-specific CD8<sup>+</sup> T-cell compartment and likely provide a benefit to MS patients in terms of both preventing demyelination and enhancing remyelination. The TMEV model provides an ideal model to address this question. To study the effects of TMEV transgenes and absence of virus capsid-specific T cells on remyelination, we chose susceptible B10.Q mice with the same H-2D<sup>q</sup> haplotype as FVB mice but show minimal remyelination [12]. We showed previously that B10.Q/β2-microglobulin deficient mice, with virtually absent CD8<sup>+</sup> T-cells, exhibit remarkable spontaneous repair [12] and have minimal neurologic deficits [10]. Therefore, we generated VP1<sup>+</sup> and VP2<sup>+</sup> transgenic mice on the same B10.Q background and designed experiments to determine which subset of T-cells directed against virus capsid antigens is responsible for influencing remyelination.

## Materials and Methods

### Mice

TMEV VP1<sup>+</sup> and VP2<sup>+</sup> transgenic mice were originally generated on FVB background as previously reported [17]. Briefly, transgenic mice were generated by cloning the coding sequence of each TMEV transgene into the eukaryotic expression vector pUB6, which contained an upstream human ubiquitin c promoter (Invitrogen, Carlsbad, CA). DNA was directionally cloned from the TMEV clone pDAFL3 using a BamHI site on the 5' end of the cloned fragment and an EcoRV site on the 3' end. The construct was cloned while maintaining the His Tag included in the vector, thereby allowing the identification of each transgene by this marker. VP2 and VP1 constructs were cut with Bgl II and Pvu II to yield fragments of 2352 and 2373 bp. The VP2 construct encoded a 279 amino acid product that included the 267 amino acids of VP2. The VP1 construct encoded a 286-amino acid product that included the 274 amino acids of VP1. All fragments were gel purified and sequenced

before injection into embryos. Gel-purified cDNA was injected into FVB embryos for implantation into pseudo-pregnant females. All embryo injections and implantations were done at the Mayo Clinic Transgenic Core Facility under the direction of Dr. Chella David. Tail samples from the offspring were used to obtain genomic DNA for determining transgene integration. Lines of VP1+ and VP2+ transgenic mice were established from mice containing the highest expression as determined by semi-quantitative PCR. DNA samples were screened using primers for the particular TMEV gene as well as the ubiquitin c promoter region. All mice used in every experiment were screened by PCR prior to their use in subsequent assays. FVB transgenic mice were then backcrossed 5 generations to B10.Q background. The presence of the VP1+ or VP2+ transgenes was confirmed in each generation by reverse transcription polymerase chain reaction (RT-PCR) [15]. After crossing was completed, the *q*-haplotype was confirmed by DNA microarray. All mice were housed and bred in Mayo Clinic's animal care facility. Animal protocols were approved by the Mayo Clinic Institutional Animal Care and Use Committee. The generation of transgenic mice, genotyping and breeding was performed by an individual independent of the person performing the subsequent experiments.

### **Theiler's virus model of demyelination**

Demyelinating disease was induced in 6- to 8-week-old mice by intracerebral injection of TMEV. A 27-gauge needle delivered 10  $\mu$ l containing  $2.0 \times 10^5$  plaque-forming units of Daniel's strain TMEV. This resulted in >98% incidence of infection with rare fatalities.

### **Brain pathology**

Brain pathology was assessed at 21, 45, 90, 180 and 270 days post infection (dpi), using our previously described technique [18]. Following perfusion with Trump's fixative, we made two coronal cuts in the intact brain at the time of removal from the skull (one section through the optic chiasm and a second section through the infundibulum). As a guide, we used the *Atlas of the Mouse Brain and Spinal Cord* corresponding to sections 220 and 350, page 6 [19]. This resulted in three blocks that were then embedded in paraffin. This allowed for systematic analysis of the pathology of the cortex, corpus callosum, hippocampus, brain stem, striatum and cerebellum. Resulting slides were then stained with hematoxylin and eosin. Each area of the brain was graded on a five-point scale as follows: 0, no pathology; 1, no tissue destruction but only minimal inflammation; 2, early tissue destruction (loss of architecture) and moderate inflammation; 3, definite tissue destruction (demyelination, parenchymal damage, cell death, neurophagia, neuronal vacuolation); and 4, necrosis (complete loss of all tissue elements with associated cellular debris). Meningeal inflammation was assessed and graded as follows: 0, no inflammation; 1, one cell layer of inflammation; 2, two cell layers of inflammation; 3, three cell layers of inflammation; 4, four or more cell layers of inflammation. The area with maximal tissue damage was used for assessment of each brain region. Pathological scores were assigned without knowledge of experimental group to the different areas of the brain.

## Spinal cord morphometry

Spinal cord morphometry was assessed in all strains at 21, 45, 90, 180 and 270 days post infection (dpi). Mice were anesthetized with sodium pentobarbital and perfused intracardially with Trump's fixative (phosphate-buffered 4% formaldehyde/1% glutaraldehyde, pH 7.4). Spinal cords were removed and sectioned precisely into 1 mm blocks. In order to represent the samples along the length of the spinal cord, every third block was post-fixed, stained with osmium tetroxide and embedded in araldite plastic (Polysciences, Warrington, PA). One-micron sections were cut and stained with 4% p-phenylenediamine to visualize the myelin sheaths. Ten spinal cord cross sections, spanning the entire spinal cord from cervical to the distal lumbar spinal column regions, were examined from each mouse. Each quadrant from every coronal section from each mouse was graded for presence of inflammation, demyelination and remyelination. Areas of demyelination were characterized by naked axons, cellular infiltration and macrophages with engulfed myelin debris. Abnormally thin myelin sheaths relative to axonal diameter and absence of Schwann cells were indicative of oligodendrocyte remyelination. Thick myelin sheaths and the one-to-one relationship between axons and Schwann cells identified Schwann cell remyelination. Areas of demyelination and remyelination were well demarcated and allowed accurate quantitative assessment at the 10 $\times$  and 40 $\times$  magnifications, respectively. The demyelination score was expressed as the percentage of spinal cord quadrants examined with the pathological abnormality. A maximum score of 100 indicated a particular pathological abnormality in every quadrant of all spinal cord sections of a given mouse. A spinal cord quadrant was considered remyelinated if greater than 75% of the axons in the field showed remyelination. Remyelination score was calculated as the ratio (%) of spinal cord quadrants with remyelination as the function of the number of spinal cord quadrants with pathologic white matter abnormalities (demyelination) that had the potential to be remyelinated. All grading was performed on coded sections without knowledge of the experimental group.

## Axon Counts

Counting of mid-thoracic (T6) axons was performed at 90, 180 at 270 days post infection. To calculate number of myelinated axons, a one-micron section was cut from the 1-mm block corresponding to mid-thoracic (T6) spinal cord section from each animal. This level was chosen because it contains both ascending and descending axons with neuronal soma in the brainstem. To ensure an identical intensity of myelin labeling, all spinal cord T6 sections used in the experiment were stained with the same batch of 4% para-phenylenediamine for exactly 20 minutes. An Olympus Provis AX70 microscope fitted with a DP70 digital camera and a 60 $\times$  oil-immersion objective was used to capture six sample areas of normal-appearing white matter containing a relative absence of demyelination from each cross section, according to the previously described sampling scheme [20]. The six fields were collected in a clockwise manner around the spinal cord in order to obtain representative samplings of the posterior-lateral, antero-lateral, and anterior columns. Images were centered between the gray matter and meningeal surface. Approximately 400,000  $\mu\text{m}^2$  of white matter was sampled from each mouse. Absolute myelinated axon numbers were calculated as previously reported [11]. After collecting six digitized images, image analysis software was used to segment the gray values (145 to 255) corresponding to the axoplasm in each image.

The batch algorithm, generated in Matlab (The Mathworks, Natick, MA), automatically quantified the number and area ( $\mu\text{m}^2$ ) of each axon from the segmented binary image after regions corresponding to vasculature, cell bodies and longitudinal axons were excluded based on circularity thresholding. Diameters less than  $1\mu\text{m}$  were excluded to eliminate structures that did not correspond to axons. Data were represented as the absolute number of all axons sampled per mid-thoracic spinal cord section. All numbers were averaged across all animals per group. The total axons from the 6 areas were then divided in three groups as a function of their caliber:  $1\text{--}3.99\mu\text{m}^2$  (small-caliber axons);  $4\text{--}10\mu\text{m}^2$  (medium-caliber axons); and  $>10\mu\text{m}^2$  (large-caliber axons). In addition, large-caliber axons were represented as a relative frequency distribution by dividing the number of these axons by the total number of sampled axons. All axon counting was performed on coded sections without knowledge of the experimental group.

## Statistics

Data were analyzed by one way ANOVA for normally distributed data, in which the Holmes-Sidak test was used for pair-wise multiple comparisons, and Kruskal-Wallis ANOVA on ranks for data that were not normally distributed, in which Dunn's test was used for pair-wise multiple comparisons. In all analyses,  $p<0.05$  was considered as statistically significant difference. We used Chi square test to compare remyelination frequency across the three groups of animals.

## Results

### VP1 and VP2 transgenes did not alter overall brain pathology in B10.Q mice

To determine whether transgenic expression of VP1 or VP2 capsid proteins had an impact on the severity of brain pathology, we assessed the pathology in brains from all transgene (VP1+ and VP2+)-positive mice and transgene-negative littermate controls. We averaged scores from all analyzed brain areas for all animals in a given group. Although some minor differences were found, pathological analysis of brains of all transgenic and wild type mice revealed no major differences in the severity of brain lesions. Only in the early disease (21 dpi) average were brain scores significantly higher in VP1+ mice compared to both transgene-negative and VP2+ mice ( $p<0.05$ , ANOVA on Ranks) (Fig. 1A). This is because few VP1+ mice had more pronounced meningeal inflammation ( $p<0.05$ , ANOVA on Ranks) (Fig. 1B). However, average brain scores and distribution of TMEV-induced lesions were similar from 45 to 270 dpi in all brain areas regardless of mouse strain. We concluded that the expression of virus transgenes did not alter the gross extent of brain pathology.

### VP1 and VP2 transgenes did not influence major differences in spinal cord inflammation and demyelination

We analyzed spinal cord samples from the same animals in order to determine whether transgenic expression of VP1 or VP2 altered pathology. Throughout the course of TMEV-induced disease, spinal cord inflammation was mostly equivalent in all three strains, with exception at 90 dpi, when transgene negative controls had more pronounced meningeal inflammation compared to both VP1+ and VP2+ mice ( $p<0.05$ , ANOVA on Ranks) (Fig. 2A). Likewise, demyelination was similar until the last time point (270 dpi), when lesion

load continued to increase in transgene negative animals, became statistically significant as compared to VP2+ animals ( $p < 0.05$ , ANOVA on Ranks) and approached significance as compared to VP1+ animals (Fig. 2B).

### **Transgenic expression of VP1 and to a lesser extent VP2 proteins resulted in increased spinal cord remyelination**

In the TMEV-mediated demyelinating disease, remyelination is usually detected from 90 dpi and later. Therefore, we analyzed three chronic time points 90, 180 and 270 dpi and consistently found more remyelination in both transgenic strains compared to transgene-negative animals ( $p < 0.05$ , ANOVA on Ranks) (Fig. 2C). Interestingly, at 270 dpi VP1+, transgenic animals showed a trend towards more remyelination than VP2+ mice but this difference did not reach statistical significance. In addition, when we analyzed animals from all three strains at 270 dpi, we found that overall VP1+ transgenic animals had more abundant remyelination (Table 1). We observed that virtually all VP1+ animals featured remyelination (10 of 10), as compared to 9 of 17 and 15 of 17 of transgene negative and VP2+ mice, respectively (Table 1). This difference was statistically significant when compared by chi-square test ( $p < 0.001$ ). Furthermore, when we used more rigorous criteria and looked at animals only with extensive remyelination ( $> 50\%$  of all demyelinated quadrants) we saw that 4 of 10 VP1+ animals fell into this category compared to none of transgene-negative and only 1 of 19 VP2+ mice (Table 1). This was also highly statistically significant by chi-square test ( $p < 0.001$ ). Figure 3 shows examples of no remyelination in transgene-negative animals (3A and B) and different qualities of remyelination in VP1+ (3C and D) and VP2+ animals (3E and F) at 270 dpi.

### **Transgenic expression of VP1 virus capsid protein resulted in relative protection of mid-thoracic axons**

Axon counts were performed in uninfected and TMEV-infected animals from all three strains at 90, 180 and 270 dpi. As expected, total number of axons in uninfected transgene negative, VP1+ or VP2+ animals was not different ( $p = 0.73$ , ANOVA) (Fig. 4A). All three strains had similar number of axons at 90 dpi. However, starting from 180 dpi differences started to emerge, as VP1+ mice tended to have more axons versus transgene negative mice. At 270 dpi, VP1+ mice, had significantly more axons than transgene negative controls ( $p = 0.02$ , ANOVA) (Fig. 4A). At this point VP1+ mice also tended to have more axons than VP2+ mice, but the difference did not reach statistical significance. In addition, we plotted the total number of mid-thoracic axons from all individual uninfected and infected animals against the corresponding time point post-infection (0–270 dpi). For all three strains we observed negative and statistically significant correlation (Fig. 4B–D). Interestingly, the slopes of lines for transgene negative (Fig. 4B) and VP2+ mice (Fig. 4D) were steeper than the line for VP1+ mice (Fig. 4C).

To study axons in more detail, we analyzed the distribution of all counted axons at 270 dpi, time point when we saw most profound difference not only in number of axons, but also in extent of remyelination. Number of small caliber axons ( $1\text{--}3.99\mu\text{m}^2$ ) was similar in all three strains (Fig. 5A). As compared to VP1+ mice, medium caliber axons ( $4\text{--}10\mu\text{m}^2$ ) were significantly decreased in both transgene negative and VP2+ animals ( $p < 0.001$ ,  $p = 0.016$ ,

respectively, pairwise ANOVA) (Fig. 4B). Interestingly, both VP1+ and VP2+ mice had more large caliber axons ( $>10\mu\text{m}^2$ ) as compared to transgene negative controls ( $p<0.001$ ,  $p=0.036$ , respectively, pairwise ANOVA) (Fig. 5C). VP1+ mice tended to have more of large-caliber axons than VP2+ mice, but this was not significant ( $p=0.09$ , pairwise ANOVA). In addition, to provide a better visual representation we plotted large caliber axons as a function of their relative frequency, and found that their distribution in transgene negative mice was distinct from VP1+ and VP2+ transgenic mice (Fig. 5D).

## Discussion

Following myelin injury and TMEV-induced demyelination, axons initially respond by redistribution of sodium channels to allow conduction of axon potential [10]. However, prolonged demyelination and metabolically unfavorable conditions lead ultimately to axon demise. Therefore, protecting axons by remyelination is critical to preserve motor, sensory and/or other neurological functions. In general, mice susceptible to TMEV-induced demyelinating disease show a spectrum from poor to remarkable remyelination [21, 22]. On one side of a spectrum, B10.Q mice feature demyelination, minimal remyelination and progressive axonal loss [12]. In contrast, the FVB strain with the same H-2<sup>q</sup> haplotype as B10.Q mice features extensive myelin repair and preserved motor function [16]. Regardless of the mechanisms of myelin repair, remyelination is clearly associated with prevention of neurological disability [10, 23]. Remyelination in the TMEV model is a late phenomenon. It starts after 3 months post TMEV-infection, when demyelination reaches a plateau, and increases in the very late phases in the disease (9–12 months post infection) [16].

In previous studies, we used transgenic expression of TMEV capsid proteins as “self” to investigate the role of CD8<sup>+</sup> T cells in virus clearance and resistance [13, 17]. The more recent study investigated the roles of CD8<sup>+</sup> T cells on the extent of spinal cord pathology and axonal loss in susceptible FVB mice showing remarkable repair [15]. Therefore, to study the effects of virus-specific CD8<sup>+</sup> T cells on remyelination, we used transgenic animals on the B10.Q background.

The major finding in this study is that the lack of CD8<sup>+</sup> T-cells specific for virus capsid protein VP1 and, to a lesser extent, VP2 enhanced remyelination, and prevented further demyelination and axonal loss. Generally, the idea that CD8<sup>+</sup> T cells have a remyelination-suppressive role is not novel. Two decades ago, Rodriguez and Lindsley demonstrated 5–7-fold increased levels of remyelination in chronically TMEV-infected mice following immunosuppression with cyclophosphamide or monoclonal antibodies that eliminated both CD4<sup>+</sup> and CD8<sup>+</sup> T cells [24]. Importantly, when only the CD4<sup>+</sup> T cell subset was depleted, remyelination was not enhanced. Subsequently, our laboratory successfully demonstrated that deletion of  $\beta$ 2-microglobulin ( $\beta$ 2m) in a poorly remyelinating strain (B10.Q) led to spontaneous and extensive remyelination [12]. Moreover, we showed that CD8<sup>+</sup> T cells were likely responsible for increased levels of demyelination in the late phase of disease in B10.Q animals [12]. Of interest, enhanced remyelination occurred in  $\beta$ 2m-deficient mice, although virus antigen and RNA persisted. This finding indicated that the demyelination and axonal injury that occur in chronic disease were immune-mediated, most likely driven by CD8<sup>+</sup> T cells. In the current study we wanted to elucidate which subset of CD8<sup>+</sup> T cells was



responsible for worsened demyelination and, more importantly, enhanced remyelination in the late disease. We showed that transgene-negative controls had more demyelination than transgene-positive animals late in the disease course. In addition, both VP1+ and VP2+ mice featured more remyelination, not only at the last time point (270 dpi), but also at 180 dpi, when demyelination levels were similar in all three strains. Interestingly, at 270 dpi, despite a notable trend toward more remyelination in VP1+ than in VP2+ mice, this difference did not reach statistical significance. However, the quality and frequency of remyelination in VP1+ mice was striking and showed high statistical significance by chi-square test when compared to VP2+ mice. Finally, when we compared the levels of remyelination in  $\beta 2m$ -deficient B10.Q mice from the previous study versus VP1+ B10.Q mice, we found identical levels of remyelination. Taken together, the data are consistent with the hypothesis that deletion of only VP1-specific CD8<sup>+</sup> T cells was sufficient to improve remyelination to the same extent as deletion of all CD8<sup>+</sup> T cells.

Another finding in this study was that early in the disease course (21 dpi) VP1+ animals had significantly more brain pathology. When we analyzed the distribution of brain lesions, we found few animals with significant meningeal inflammation, which led to a higher overall brain pathological score. We do not believe that this is biologically significant as overall brain scores and lesion distribution were similar between 45 to 270 dpi. However, we cannot exclude the possibility that at 21 dpi, the lack of VP1-specific CD8<sup>+</sup> T cells was responsible for more meningeal inflammation in a few animals.

When we counted axons at 270 dpi we observed higher axon density in VP1+ mice versus both transgene-negative and VP2+ mice, due to more medium- and large-caliber axons in VP1+ mice. The difference in number of axons between VP1+ and transgene-negative mice likely comes as a consequence of both enhanced remyelination and less demyelination in VP1 strain. On the other hand, the difference in axon density between VP1+ and VP2+ mice was predominantly due to more complete and more frequent remyelination in the VP1 strain, as demyelination was similar in both strains. When we plotted mid-thoracic axons against the specific time point in the disease, we observed negative and statistically significant correlation. This is consistent with the observation that progressive axonal loss occurs in TMEV-induced demyelinating disease. However, we showed that the correlation line between axonal dropout and dpi in VP1+ mice was less steep than lines in transgene-negative and VP2+ mice. This finding supported relative axonal protection and more remyelination in VP1+ animals.

During the last several years, an increasing body of literature reveals important roles for regulatory CD8<sup>+</sup> T cells, and especially axon-damaging IL-17-secreting CD8<sup>+</sup> T cells [25]. Using a transgenic approach that eliminated all of CD8<sup>+</sup> T cells specific for VP1 or VP2 capsid proteins, we cannot pinpoint which subset of CD8<sup>+</sup> T cells is critical in preventing remyelination. Future studies are needed to characterize precisely regulatory and IL-17-secreting CD8<sup>+</sup> T cells, which will hopefully allow targeted removal of these discrete cell subsets and help in elucidating their individual roles.

In summary, using the virus-induced model of demyelinating disease in mice, we provide additional evidence that the adaptive immune response, predominantly CD8<sup>+</sup> T cells

directed against VP1 and to a lesser extent VP2 capsid proteins, is responsible for inhibiting myelin regeneration in TMEV-induced demyelination in B10.Q mice. In the demyelination setting, specific CD8<sup>+</sup> T cells are not only the main culprits in axonal transection and injury but also represent the factor that limits or prevents naturally occurring process of myelin repair. In support of this concept is the spontaneously occurring remyelination in two toxin-induced models of demyelination, the lyssolecithin and cuprizone models, due to absence of an immune response to the toxin. However, in a virus-induced, immune-mediated demyelinating disease, tampering with the immune function, i.e., removal of VP1+ specific CD8<sup>+</sup> T cells led to enhanced CNS remyelination.

The best supporting evidence for the importance of CD8<sup>+</sup> T cells in human MS is several landmark studies on autopsy lesion samples as well as recent clinical trials. It is clear that regardless of disease phase, CD8<sup>+</sup> T cells consistently outnumber CD4<sup>+</sup> T cells and are clonally expanded in inflammatory infiltrates found in MS lesions [7, 8, 26]. Furthermore, whereas treatment with anti-CD4 monoclonal antibody did not yield a beneficial effect [27], treatments with natalizumab [28] and alemtuzumab [29], drugs that affect both CD4<sup>+</sup> and CD8<sup>+</sup> T cells, provided a significant therapeutic effect. Unfortunately, by preventing the migration of all T cells into the CNS, natalizumab, in rare cases, causes opportunistic infection with JC virus and a fatal progressive multifocal leukoencephalopathy [30]. Taken together, the results from our study provides strong support that, once an antigen or groups of antigens that cause MS are identified, targeted removal of antigen-specific CD8<sup>+</sup> T cells will likely provide a great benefit to MS patients and eliminate the opportunistic infections as a consequence of pan-CD8<sup>+</sup> T cell depletion.

## Acknowledgments

This work was supported by grants from the NIH (R01 GM092993, R01 NS048357 and R21 NS073684) and the National Multiple Sclerosis Society (CA 1060A). This work was also supported by a High-Impact Pilot and Feasibility Award (HIPFA) and Novel Methodology Award (NMDA) from the Mayo Clinic Center for Translational Science Activities (CTSA), Mayo Clinic CTSA grant number UL1 TR000135 from the National Center for Advancing Translational Science (NCATS), a component of the National Institutes of Health (NIH) and Investigator-initiated protocol award from Center for Multiple Sclerosis and Demyelinating Diseases (CMSDD). We also acknowledge with thanks support from the Applebaum, Hilton, Peterson and Sanford Foundations, the Minnesota Partnership Award for Biotechnology and Medical Genomics and the McNeilus family.

## References

1. Lassmann H, Bruck W, Lucchinetti C, Rodriguez M. Remyelination in multiple sclerosis. *Mult Scler.* 1997; 3(2):133–6. [PubMed: 9291167]
2. Prineas JW, Kwon EE, Goldenberg PZ, Ilyas AA, Quarles RH, Benjamins JA, et al. Multiple sclerosis. Oligodendrocyte proliferation and differentiation in fresh lesions. *Lab Invest.* 1989; 61(5): 489–503. [PubMed: 2811298]
3. Raine CS, Traugott U. Chronic relapsing experimental autoimmune encephalomyelitis. Ultrastructure of the central nervous system of animals treated with combinations of myelin components. *Lab Invest.* 1983; 48(3):275–84. [PubMed: 6186840]
4. Denic A, Johnson AJ, Bieber AJ, Warrington AE, Rodriguez M, Pirko I. The relevance of animal models in multiple sclerosis research. *Pathophysiology.* 2011; 18(1):21–9.10.1016/j.pathophys.2010.04.004 [PubMed: 20537877]
5. Kappos L, Comi G, Panitch H, Oger J, Antel J, Conlon P, et al. Induction of a non-encephalitogenic type 2 T helper-cell autoimmune response in multiple sclerosis after administration of an altered

- peptide ligand in a placebo-controlled, randomized phase II trial. The Altered Peptide Ligand in Relapsing MS Study Group. *Nat Med.* 2000; 6(10):1176–82.10.1038/80525 [PubMed: 11017151]
6. Bielekova B, Goodwin B, Richert N, Cortese I, Kondo T, Afshar G, et al. Encephalitogenic potential of the myelin basic protein peptide (amino acids 83–99) in multiple sclerosis: results of a phase II clinical trial with an altered peptide ligand. *Nat Med.* 2000; 6(10):1167–75.10.1038/80516 [PubMed: 11017150]
  7. Babbe H, Roers A, Waisman A, Lassmann H, Goebels N, Hohlfeld R, et al. Clonal expansions of CD8(+) T cells dominate the T cell infiltrate in active multiple sclerosis lesions as shown by micromanipulation and single cell polymerase chain reaction. *J Exp Med.* 2000; 192(3):393–404. [PubMed: 10934227]
  8. Skulina C, Schmidt S, Dornmair K, Babbe H, Roers A, Rajewsky K, et al. Multiple sclerosis: brain-infiltrating CD8+ T cells persist as clonal expansions in the cerebrospinal fluid and blood. *Proc Natl Acad Sci U S A.* 2004; 101(8):2428–33. [PubMed: 14983026]
  9. Theiler M. Spontaneous Encephalomyelitis of Mice—a New Virus Disease. *Science.* 1934; 80(2066):122.10.1126/science.80.2066.122-a [PubMed: 17750712]
  10. Rivera-Quinones C, McGavern D, Schmelzer JD, Hunter SF, Low PA, Rodriguez M. Absence of neurological deficits following extensive demyelination in a class I-deficient murine model of multiple sclerosis. *Nat Med.* 1998; 4(2):187–93. [PubMed: 9461192]
  11. Howe CL, Adelson JD, Rodriguez M. Absence of perforin expression confers axonal protection despite demyelination. *Neurobiol Dis.* 2007; 25(2):354–9.10.1016/j.nbd.2006.10.001 [PubMed: 17112732]
  12. Denic A, Pirko I, Wootla B, Bieber A, Macura S, Rodriguez M. Deletion of beta-2-microglobulin ameliorates spinal cord lesion load and promotes recovery of brainstem NAA levels in a murine model of multiple sclerosis. *Brain Pathol.* 2012; 22(5):698–708.10.1111/j.1750-3639.2012.00576.x [PubMed: 22335434]
  13. Lin X, Njenga MK, Johnson AJ, Pavelko KD, David CS, Pease LR, et al. Transgenic expression of Theiler's murine encephalomyelitis virus genes in H-2(b) mice inhibits resistance to virus-induced demyelination. *J Virol.* 2002; 76(15):7799–811. [PubMed: 12097592]
  14. Yauch RL, Kim BS. A predominant viral epitope recognized by T cells from the periphery and demyelinating lesions of SJL/J mice infected with Theiler's virus is located within VP1(233–244). *J Immunol.* 1994; 153(10):4508–19. [PubMed: 7525707]
  15. Denic A, Zoecklein L, Kerkvliet J, Papke L, Edukulla R, Warrington A, et al. Transgenic expression of viral capsid proteins predisposes to axonal injury in a murine model of multiple sclerosis. *Brain Pathol.* 2011; 21(5):501–15.10.1111/j.1750-3639.2011.00474.x [PubMed: 21314744]
  16. Bieber AJ, Ure DR, Rodriguez M. Genetically dominant spinal cord repair in a murine model of chronic progressive multiple sclerosis. *J Neuropathol Exp Neurol.* 2005; 64(1):46–57. [PubMed: 15715084]
  17. Pavelko KD, Pease LR, David CS, Rodriguez M. Genetic deletion of a single immunodominant T-cell response confers susceptibility to virus-induced demyelination. *Brain Pathol.* 2007; 17(2):184–96.10.1111/j.1750-3639.2007.00062.x [PubMed: 17388949]
  18. Pavelko KD, Howe CL, Drescher KM, Gamez JD, Johnson AJ, Wei T, et al. Interleukin-6 protects anterior horn neurons from lethal virus-induced injury. *J Neurosci.* 2003; 23(2):481–92. [PubMed: 12533608]
  19. Sidman, RL.; Angevine, JB.; Pierce, ET. Atlas of the mouse brain and spinal cord. Harvard Univ Press; 1971.
  20. Denic A, Bieber A, Warrington A, Mishra PK, Macura S, Rodriguez M. Brainstem (1)H nuclear magnetic resonance (NMR) spectroscopy: Marker of demyelination and repair in spinal cord. *Annals of neurology.* 2009; 66(4):559–64. [PubMed: 19816926]
  21. McGavern DB, Murray PD, Rodriguez M. Quantitation of spinal cord demyelination, remyelination, atrophy, and axonal loss in a model of progressive neurologic injury. *J Neurosci Res.* 1999; 58(4):492–504. [PubMed: 10533042]
  22. Sathornsumetee S, McGavern DB, Ure DR, Rodriguez M. Quantitative ultrastructural analysis of a single spinal cord demyelinated lesion predicts total lesion load, axonal loss, and neurological

- dysfunction in a murine model of multiple sclerosis. *Am J Pathol.* 2000; 157(4):1365–76.10.1016/S0002-9440(10)64650-0 [PubMed: 11021839]
23. Ure DR, Rodriguez M. Preservation of neurologic function during inflammatory demyelination correlates with axon sparing in a mouse model of multiple sclerosis. *Neuroscience.* 2002; 111(2): 399–411. [PubMed: 11983325]
  24. Rodriguez M, Lindsley MD. Immunosuppression promotes CNS remyelination in chronic virus-induced demyelinating disease. *Neurology.* 1992; 42(2):348–57. [PubMed: 1736164]
  25. Denic A, Wootla B, Rodriguez M. CD8(+) T cells in multiple sclerosis. *Expert Opin Ther Targets.* 2013; 17(9):1053–66.10.1517/14728222.2013.815726 [PubMed: 23829711]
  26. Monteiro J, Hingorani R, Pergolizzi R, Apatoff B, Gregersen PK. Clonal dominance of CD8+ T-cell in multiple sclerosis. *Ann N Y Acad Sci.* 1995; 756:310–2. [PubMed: 7645848]
  27. van Oosten BW, Lai M, Hodgkinson S, Barkhof F, Miller DH, Moseley IF, et al. Treatment of multiple sclerosis with the monoclonal anti-CD4 antibody cM-T412: results of a randomized, double-blind, placebo-controlled, MR-monitored phase II trial. *Neurology.* 1997; 49(2):351–7. [PubMed: 9270561]
  28. Polman CH, O'Connor PW, Havrdova E, Hutchinson M, Kappos L, Miller DH, et al. A randomized, placebo-controlled trial of natalizumab for relapsing multiple sclerosis. *N Engl J Med.* 2006; 354(9):899–910.10.1056/NEJMoa044397 [PubMed: 16510744]
  29. Coles AJ, Compston DA, Selmaj KW, Lake SL, Moran S, Margolin DH, et al. Alemtuzumab vs. interferon beta-1a in early multiple sclerosis. *N Engl J Med.* 2008; 359(17):1786–801.10.1056/NEJMoa0802670 [PubMed: 18946064]
  30. Linda H, von Heijne A, Major EO, Ryschkewitsch C, Berg J, Olsson T, et al. Progressive multifocal leukoencephalopathy after natalizumab monotherapy. *N Engl J Med.* 2009; 361(11): 1081–7.10.1056/NEJMoa0810316 [PubMed: 19741229]

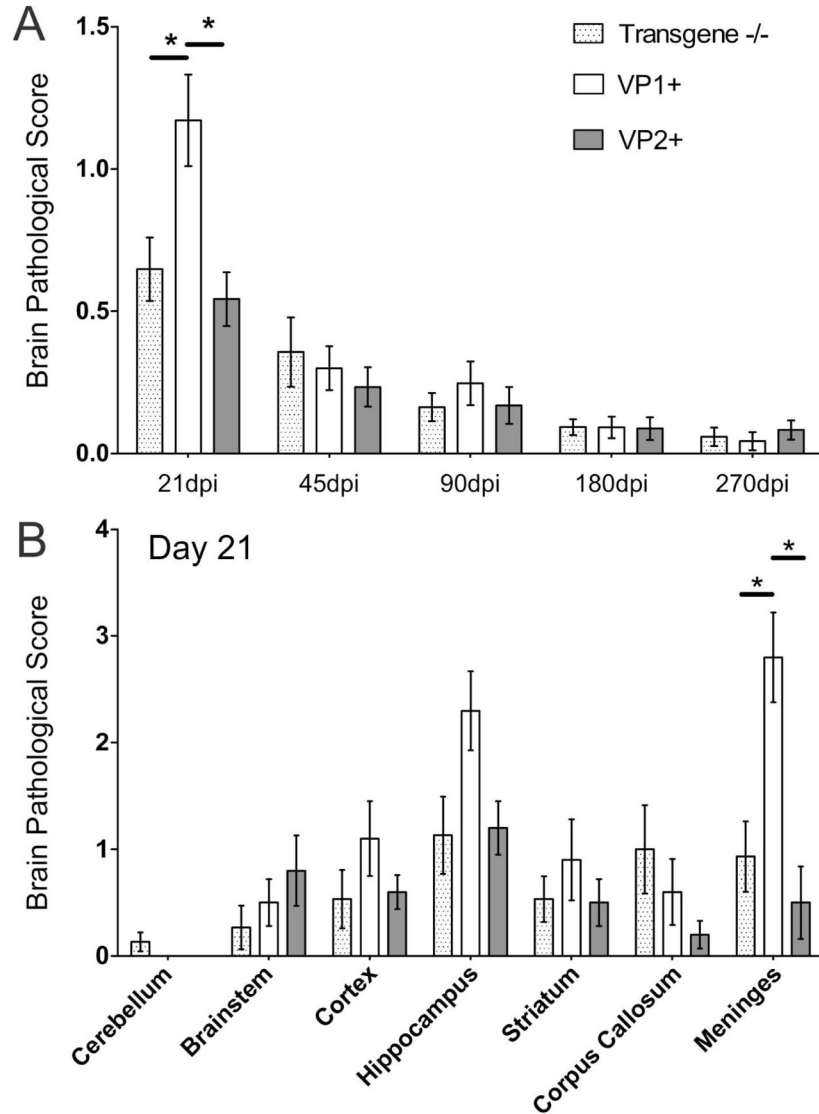


**Figure 1. Time course of brain pathology scores in B10.Q transgene negative, VP1+ and VP2+ transgenic mice following TMEV infection**

Seven areas of the brain (cerebellum, brain stem, cortex, hippocampus, striatum, corpus callosum, and meninges) were graded independently based on a five-point scale as described in the methodology section. **A**) No major differences in brain pathology were observed throughout the disease course, except at 21 dpi when VP1+ animals had higher scores ( $p < 0.05$ , ANOVA on Ranks). Scores from all areas were averaged and plotted as shown. **B**) When we looked individual scores across different brain regions, we observed that the difference at 21 dpi was driven by significantly worse scores in the meninges of several VP1+ animals. Likewise, a few VP1+ animals had higher scores in hippocampus, but this difference did not reach statistical significance. Stars denote statistical significance ( $p < 0.05$ , ANOVA on Ranks).

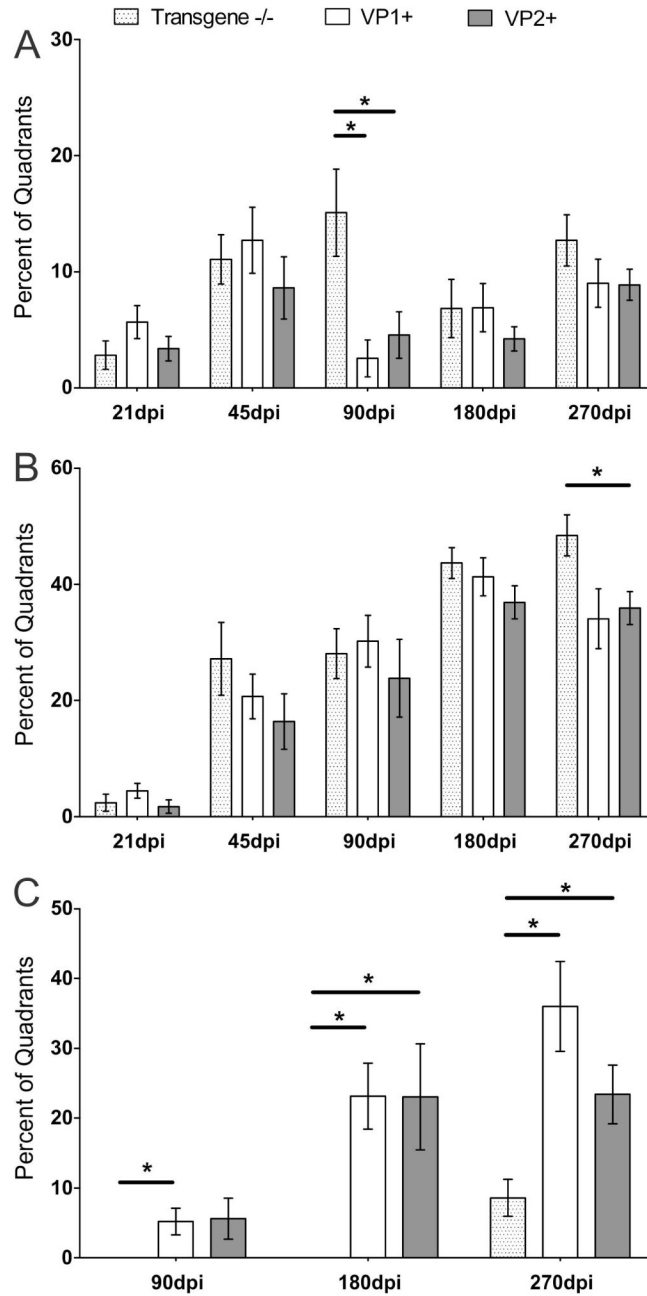


**Figure 2. Percent of spinal cord quadrants containing spinal cord white matter inflammation, demyelination and remyelination**

(A, B) All animals showed spinal cord inflammation and progressive demyelination from 21 dpi and later. No major differences were observed in inflammation or demyelination at all analyzed time points post infection. Only at 90 dpi transgene-negative controls had more meningeal inflammation ( $p < 0.05$ , ANOVA on Ranks) and more demyelination at 270dpi ( $p < 0.05$ , ANOVA on Ranks). Data expressed as a percentage of quadrants with the inflammation/demyelination as a function of all spinal cord quadrants examined. (C) At all chronic time points, 90, 180 and 270 dpi, remyelination was more pronounced in VP1+ and

VP2+ mice ( $p < 0.05$  at 90 dpi, and  $p < 0.001$  at 180 and 270 dpi, ANOVA on Ranks). In addition, at 270 dpi, VP1+ animals showed a trend towards more remyelination compared to VP2+ animals. Stars denote statistical significance.

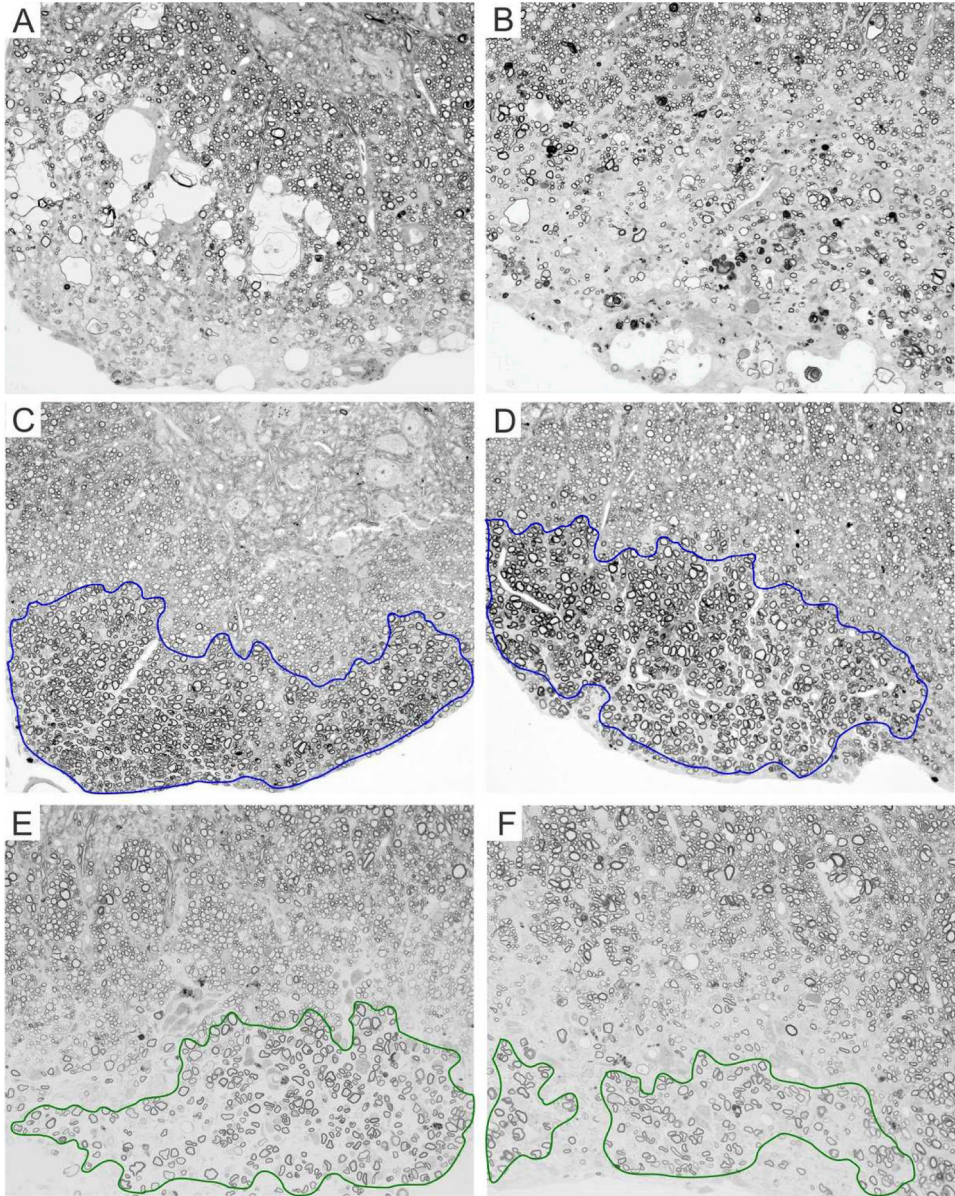


**Figure 3. Remyelination at 270 dpi is more extensive in VP1+ mice than in VP2+ and transgene negative mice**  
(A, B) Example of demyelination with no remyelination in transgene negative mice. (C, D) Examples of extensive remyelination in VP1+ mice are outlined in blue. (E, F) Examples of patchy, incomplete remyelination in VP2+ mice are outlined in green. Images were taken from anterior (A, C and E) and lateral (B, D and F) thoracic spinal cord columns, areas with prominent demyelination.



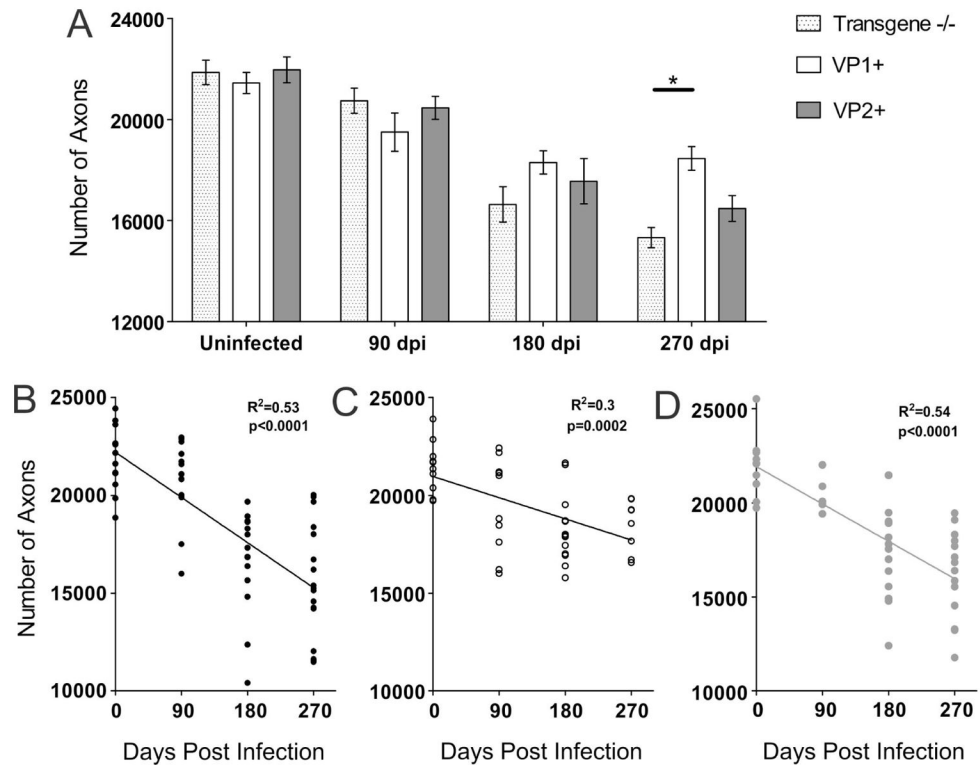


#### Figure 4. Mid-thoracic (T6) axons quantitation

Axons were counted in 6 areas of a mid-thoracic spinal cord section, as described in the methods. (A) The total number of myelinated mid-thoracic (T6) axons in mice from all three strains prior to infection and at 90 and 180 dpi was similar. At 270 dpi, VP1+ animals had significantly more axons than transgene negative mice ( $p=0.02$ , ANOVA). Bars represent the means of the group with standard error of the mean. (B–D) When the total number of axons from all transgene negative (B), VP1+ (C) and VP2+ mice (D) was plotted against time point post-infection negative and statistically significant correlations were observed. Note the steeper slopes in transgene negative and VP2+ mice as a result of overall greater axonal loss in these strains.

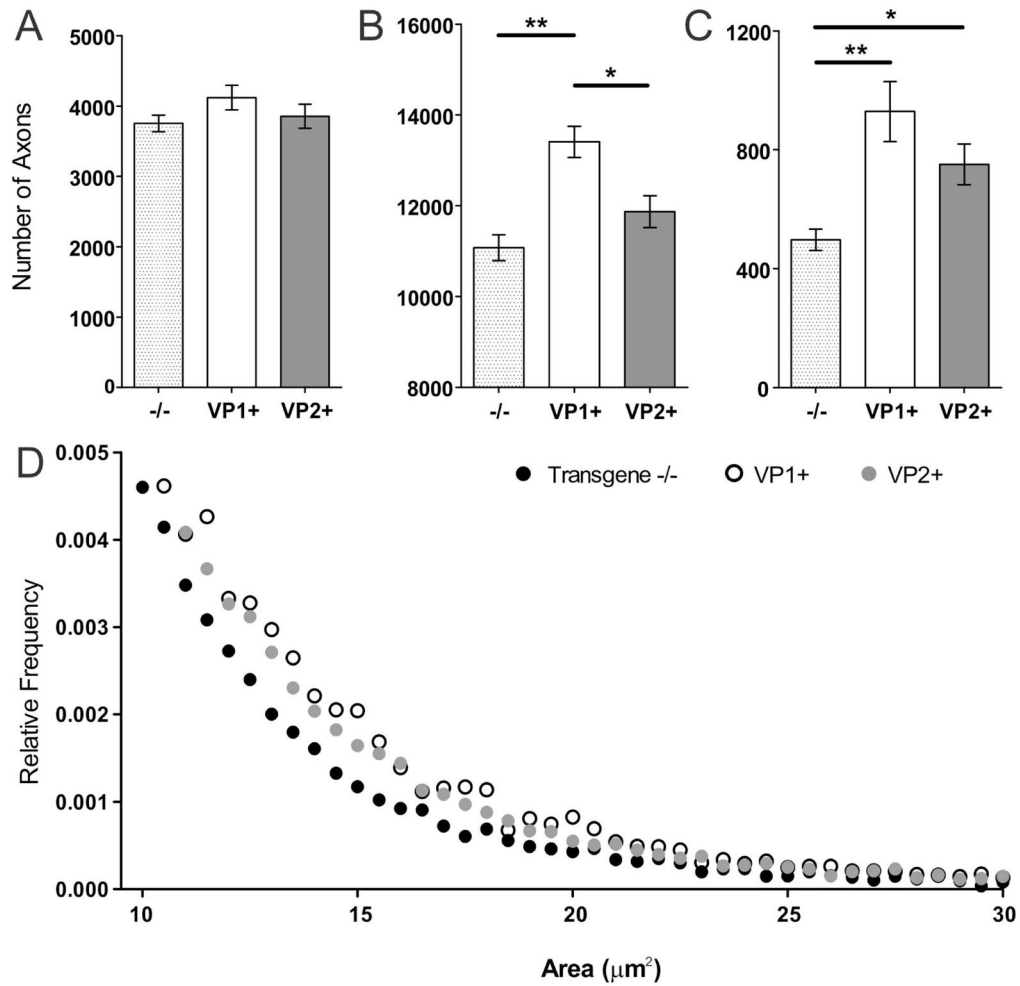


### Figure 5. Axon distributions

Total number of mid-thoracic axons from all three strains at 270 dpi were morphologically analyzed by stratifying them into three groups as a function of axons caliber (1–3.99  $\mu\text{m}^2$  small, 4–10  $\mu\text{m}^2$  medium, >10  $\mu\text{m}^2$  large). (A) In all three strains number of small caliber axons was not different ( $p=0.24$ , ANOVA). (B) However, VP1+ animals had more medium caliber axons than transgene negative controls and VP2+ mice ( $p<0.001$  and  $p=0.016$  respectively). (C) Both VP1+ and VP2+ animals had more large caliber axons than transgene negative controls ( $p<0.001$  and  $p=0.036$  respectively). Star denotes statistical significance (\*  $p<0.05$ , \*\*  $p<0.001$ ). (D) Relative frequency distribution of large caliber axons (>10  $\mu\text{m}^2$ ) across all three strains. The circles represent the relative frequency of large caliber axons using 0.5  $\mu\text{m}^2$  intervals as bins. Note the tail of axon distribution in transgene negative mice which is distinct and lower as compare to VP1+ and VP2+ mice.

**Table 1**

Frequency of remyelination at 270 dpi across three strains

Number of animals with remyelination/Total number of animals in group			
	Transgene $-/-$	VP1+	VP2+
Any Remyelination	9/17	10/10	15/19
Remyelination >50%	0/17	4/10	1/19